Proc. Natl. Acad. Sci. USA
Vol. 82, pp. 6153–6157, September 1985
Cell Biology

Visualization of the protein associations in the erythrocyte membrane skeleton

(cytoskeleton/spectrin/actin)

TIMOTHY J. BYERS AND DANIEL BRANTON

Department of Cellular and Developmental Biology, Harvard University, Cambridge, MA 02138

Contributed by Daniel Branton, May 20, 1985

ABSTRACT **We have obtained clear images of the erythrocyte membrane skeleton from negatively stained preparations that originate directly from the intact cell but in which the spectrin meshwork is artificially spread to allow close inspection. Our procedure requires less than 2 min at 5°C in phosphate buffers. We find 200-nm-long spectrin tetramers crosslinked by junctional complexes. Each junction contains a regular 37-nm rod, probably an actin oligomer of approximately 13 monomers. Densities appear at variable places in the meshwork but distinct globules occur with great frequency 78 nm from the spectrin tetramer's junctional insertion end, very close to the known binding site for ankyrin. Most frequently, five or six spectrin tetramers insert into each junction, producing a meshwork that displays remarkably regular long range order.**

Electron micrographs of the isolated mammalian erythrocyte cytoskeleton have demonstrated the existence of a continuous reticulum underlying the membrane (1, 2) but have not provided high-resolution information about the details of the structure and connections within this membrane skeleton. Although aspects of the skeleton have been visualized in thin sections of the erythrocyte ghost (3, 4), a major problem when examining the intact erythrocyte membrane or its skeleton is that the high density of proteins makes it very difficult to visualize the individual macromolecules and their connections.

The erythrocyte membrane skeleton is believed to consist of a cross-linked meshwork consisting of spectrin, actin, band 4.1, and other associated proteins. Two linkages are viewed as essential for the integrity of this meshwork: first, spectrin heterodimers must associate head to head to form tetramers and, second, tail ends of the tetramers must crosslink the meshwork by binding to junctions that include short actin oligomers and band 4.1 protein. This view of the membrane skeleton has come from studying individual purified molecules and their modes of association *in vitro* (5–9). While these studies have told us much about the shapes of the individual molecules and the affinities and positions of their binding sites, evidence that the assemblies that have been created *in vitro* duplicate the connections that exist *in situ* is limited.

Aspects of the *in situ* cytoskeletal structure have been revealed in partially dissociated membrane skeletons. Erythrocyte skeletons treated to dissociate the tails of spectrin from their association with band 4.1 and actin while preserving spectrin's head-to-head associations suggest that spectrin tetramers and medium-sized oligomers coexist in the normal erythrocyte membrane as the primary native spectrin species (10). Complementary studies of fragments produced under conditions that destroy the oligomeric associations at the head end of the spectrin molecules but preserve the associations with actin and band 4.1 at the tail end of spectrin have also been performed (11). The resultant electron micrographs showed fragments containing variable-length actin filaments and globules from which several convoluted filaments of spectrin projected.

Although some of the earliest microscopic images of the intact erythrocyte membrane skeleton were obtained by negative staining (1, 2), in only one micrograph published by Pinder *et al.* (12) can one see individual spectrin tetramers and fragmentary hints of the band 4.1–actin oligomer junctions. We have now obtained clear images of the spectrin meshwork from negatively stained preparations that originate directly from the intact cell but in which the spectrin filaments are artificially spread to allow close inspection.

MATERIALS AND METHODS

Grid Preparation. To produce holey films, a solution of 0.4% formvar in ethylene dichloride was applied to a clean glass microscope slide, drained, and allowed to dry in a humid chamber. The film was then floated onto water. Uniform films were produced as described (13). In either case, 200-mesh copper grids were placed on the floating film and lifted from above. The films were then coated with approximately 0.8 nm of carbon and subjected to glow discharge just before use.

Membrane Skeleton Preparation. The grids, mounted for convenience on coverslips (unpublished work), were treated with 0.2% (wt/wt) poly(L-lysine), M_r >300,000 (Sigma) for 1 min and extensively rinsed with phosphate-buffered saline containing Mg and EGTA (P_i/NaCl/Mg; 150 mM NaCl/5 mM NaH_2PO_4/2 mM NaN_3/2 mM $MgCl_2$/1 mM EGTA, pH 7.5) Human erythrocytes were obtained from a pricked finger, washed three times with P_i/NaCl/Mg stored at 4°C and used within 3 days. All buffers and stain were stored on ice until used but grids were manipulated in a room at 20°C. A droplet containing the washed cells was placed on a polylysine-treated grid for 30 sec and the nonadherent erythrocytes were washed off with P_i/NaCl/Mg. The adherent cells were treated with a 5 mM phosphate buffer containing Mg and EGTA (5 mM PO_4/Mg: 5 mM NaH_2PO_4/2 mM $MgCl_2$/1 mM EGTA, pH 7.5) for 10 sec then broken open with a jet of the same buffer from a 26-gauge needle at an oblique angle. The grids were washed briefly with P_i/NaCl/Mg and fixed in P_i/NaCl/Mg, pH 7.5, containing 0.1% glutaraldehyde for 5 min with mild agitation. The cells were again rinsed briefly with P_i/NaCl/Mg, negatively stained by dripping 2% uranyl acetate in distilled water over the grids for 10 sec, then blotting off excess stain. A slightly different protocol, which we found enhanced spreading of the membrane skeleton meshwork, was used for some preparations. Erythrocytes were applied to grids as above and washed with P_i/NaCl/Mg, pH 5.5, for 30 sec. Adherent cells were then treated with 5 mM PO_4/Mg, pH 5.5, for 10 sec, broken open as above with a jet of 5 mM PO_4/Mg, pH 5.5, plus 0.1% Triton X-100,

The publication costs of this article were defrayed in part by page charge payment. This article must therefore be hereby marked "*advertisement*" in accordance with 18 U.S.C. §1734 solely to indicate this fact.

washed briefly in P_i/NaCl/Mg and either negatively stained with 2% uranyl acetate or incubated with G-actin and then negatively stained.

Incubation with G-Actin. Five microliters of freshly gel-filtered G-actin at 0.2 mg/ml (14, 15) in column buffer (2 mM Tris·HCl/0.2 mM ATP/0.2 mM $CaCl_2$/0.5 mM dithiothreitol/2 mM NaN_3, pH 8.0) was mixed with 45 μl of polymerization buffer (150 mM NaCl/5 mM NaH_2PO_4/2 mM NaN_3/0.5 mM $MgCl_2$/1 mM EGTA/0.05 mM dithiothreitol, pH 7.5) just before use. A fresh drop of this mixture was pipetted onto the spread membrane skeleton preparations (as above), every minute for 3 min. The grids were then rinsed with P_i/NaCl/Mg, pH 7.5, and negatively stained with 2% uranyl acetate.

RESULTS

In our procedure, a forceful jet of medium blows away the upper surface and cytoplasm of hypotonically swollen or lysed erythrocytes, resulting in a layer of single membranes adhering to the grid substrate. After fixation and negative staining, these single membranes displayed a variable and complex appearance with few readily discernible features (Fig. 1 *a* and *b*). We refer to this image as "intact" to distinguish it from membranes in the same preparations where the integrity of the membrane skeleton was disrupted and a spread pattern of filaments began to emerge (Fig. 1*c*).

Spread Meshworks. In some of the membranes much of the membrane skeleton material appeared to be drawn or contracted into dense accumulations revealing a cleanly spread filamentous meshwork between the dense areas (Fig. 2). The spread meshwork seemed to be fixed in a state of tension; breakage and detachment was evident in maximally extended regions.

The spread meshworks were most extensive and frequent when the membrane layers were prepared with pH 5.5 buffers on grids coated with holey Formvar and carbon. A lower yield of the same spread filament images was obtained using buffers at pH 7.5. Similarly, Triton X-100 (see *Materials and Methods*) helped to give cleaner preparations but the same images were obtained without detergent and with or without fixation. Formvar films prepared by the method of Davison and Colquhoun (13) provided the best resolution and contrast. Holey films were used in some cases because the spreading phenomenon seemed to be stimulated by imperfections in the substrate but skeleton material that spanned the holes was usually distorted or fragile and is not presented here.

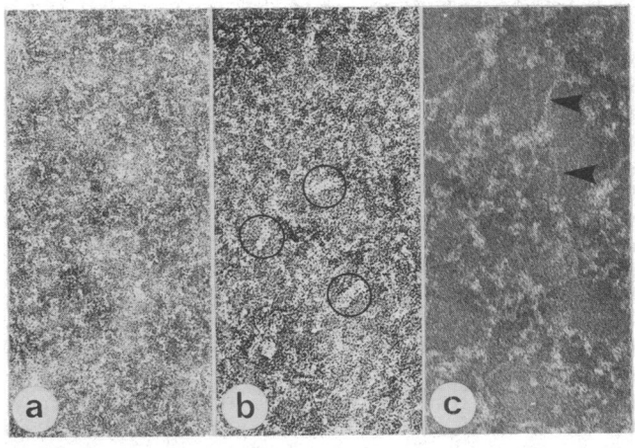

FIG. 1. Intact and partially spread membrane skeletons. The appearance of unspread negatively stained preparations (*a* and *b*) varied; in many cases short rods, *ca.* 37 nm long, were evident (circles) among a complex tangle of finer strands. The skeleton of other cells in the same preparation (*c*) appeared to have begun to spread, revealing more readily discernible individual filaments (arrowheads). (×145,500.)

The meshwork consisted of junctional complexes cross-linked by long flexible molecules that appeared to be made up of two intertwined subunits (Fig. 2). Between four and seven (average 5.3, $n = 140$) of these long molecules inserted into each junction. We believe that the long molecules are spectrin because the morphology of the elongated molecules and their length when maximally extended (203 ± 13 nm, SD, $n = 113$) matched the characteristic morphology and length of pure spectrin tetramers in rotary-shadowed preparations (16). Furthermore, the long molecules were the most prevalent element of the spread meshwork and spectrin is the major protein of the erythrocyte membrane skeleton. Distinct globules were often associated with the spectrin tetramers (Fig. 2 *b–g*). When the spectrin was maximally spread, these globules appeared 78 ± 7 nm ($n = 72$) from the ends of the spectrin molecules that inserted into the junctional complexes. When two globules were seen on one spectrin tetramer (Fig. 2 *f* and *g*) they were located 44 ± 3 nm ($n = 22$) from each other along the spectrin molecule. The distances between junction and globule and between two globules on one spectrin coincide with analogous measurements that have been made with purified rotary-shadowed spectrin reassociated with ankyrin (17), where the distance from the tail end of spectrin to its ankyrin binding site is *ca.* 80 nm and the distance between two ankyrin molecules on one spectrin tetramer is *ca.* 40 nm. It is therefore very probable that the globules seen in our negatively stained preparations are occupied ankyrin binding sites.

The junctional complexes exhibited a variable number of components (Fig. 3). A short rod, approximately 9 nm wide and 37 ± 3 nm long ($n = 103$) was the dominant element of each junction. We believe the rods to be short F-actin oligomers for the following reasons: (*i*) they appeared to be attached to spectrin, (*ii*) although the substructure of these rods was often obscured by other elements of the complex, a morphology characteristic of the F-actin filament was sometimes evident (Fig. 3), and (*iii*) the rods acted as nucleating sites for the elongation of actin filaments *in vitro* when the spread membrane skeletons were incubated with freshly gel-filtered G-actin under conditions sufficient for filament elongation (Fig. 4). Control experiments showed that the concentration of G-actin was below that necessary for significant nucleation during the 3-min incubation period we used: glow-discharged control grids without polylysine and without membrane skeletons did not show the presence of actin filaments when incubated with G-actin in polymerization buffer.

The Intact Membrane Skeleton. With a knowledge of the actin oligomer morphology gained from the spread meshwork we could identify similar short rods in the intact skeletons (Fig. 1*b*, circles). Although their boundaries were often obscured by the density of the spectrin meshwork, the average length of these rods (37 ± 5 nm, $n = 20$) and their width were similar to that of the actin oligomer seen in the spread membrane skeletons. We have counted between 90 and 210 oligomers per μm^2 in randomly selected areas of intact negatively stained preparations. These counts probably underestimate the density of oligomers because the rods are sometimes difficult to discern and partially spread regions may be present in the "intact" skeletons.

DISCUSSION

Our results provide clear and direct visual evidence for the organization of the erythrocyte membrane skeleton. While in general confirming models based on the examination of

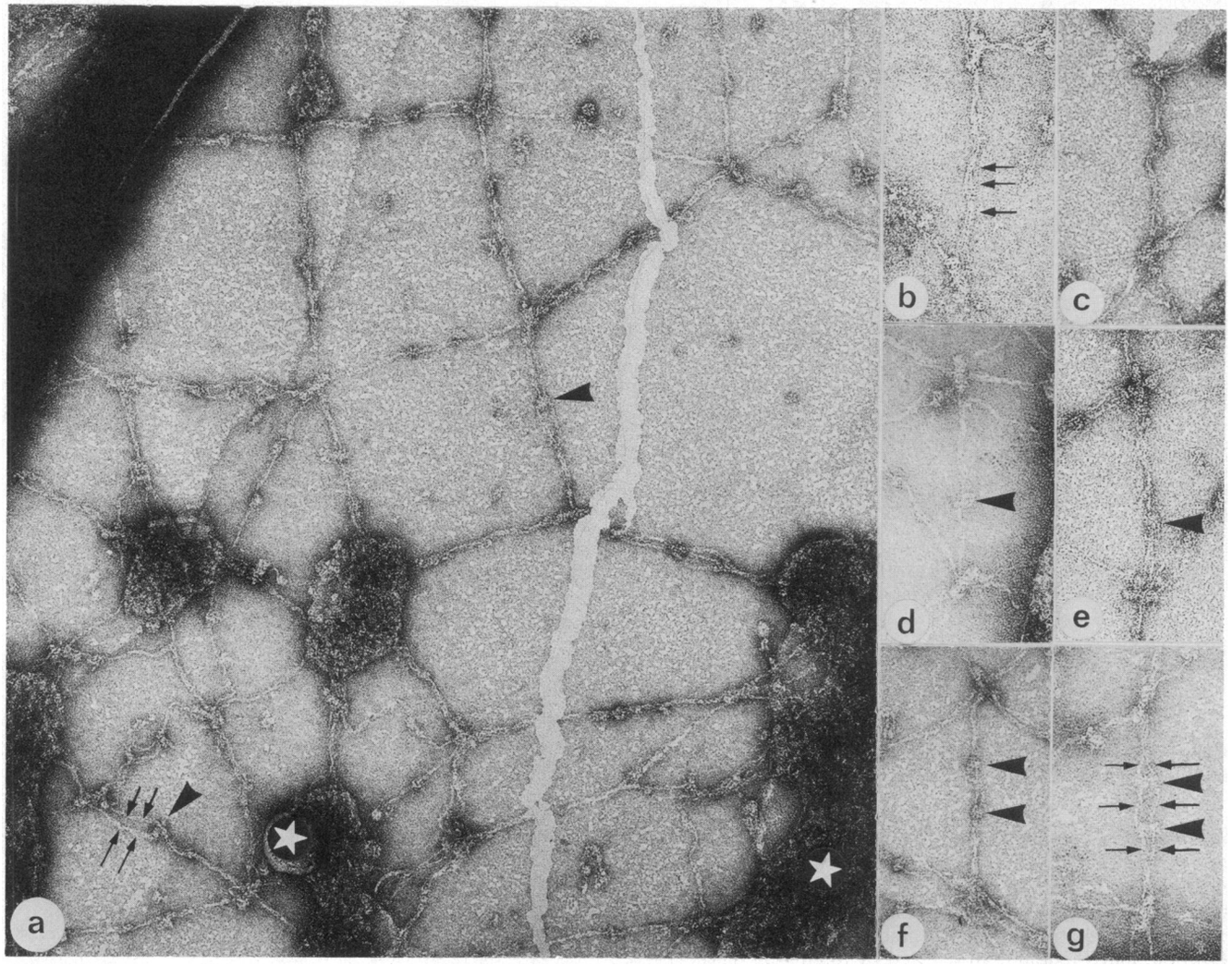

FIG. 2. Spread membrane skeletons. (*a*) A meshwork is formed by long spectrin tetramers joined at their ends by junctional complexes. In some places the individual spectrin monomer chains may be discerned, either twined around each other (single arrows, *b*) or lying side by side, separated from each other (opposed paired arrows, *a* and *g*). The spectrin is either bare (*b* and *c*) or associated with one (*d* and *e*) or a pair (*f* and *g*) of distinct globules (arrowheads) *ca.* 78 nm from the junctions. Surrounding and interspersed with the spread meshwork are dense regions of accumulated membrane skeleton material (stars). (×150,000.)

partially dissociated membrane skeletons (10, 11) and on the *in vitro* behavior of purified components (6, 9), our views of spread membrane skeletons provide previously unavailable information about the packing of spectrin on the membrane and the organization of the junctional complexes.

An average of five or six spectrin tetramers radiate from the junctional complexes, but in every case where the images are clear we observed only one tetramer extending between any two neighboring junctional complexes. In many cases the membrane skeleton was spread to the extent that the end-to-end length of the spectrin strands was equivalent to the known (16) 194 ± 15 nm contour length of a spectrin tetramer. Our ability to spread the meshwork to this extent without apparently destroying junction-to-junction connections indicates that *in situ* the packed spectrin chains are not entangled in a manner that requires topological alterations to effect a metric change.

Medium-sized spectrin oligomers of three or more heterodimers can account for more than 25% of the spectrin in the native membrane (10, 18). Our images to date may not distinguish individual tetramers from molecules that are part of higher order oligomers. A molecule that extends between any two junctions is a tetramer in the sense that it is composed of two β and two α chains. But if the equilibrium of the head-to-head interactions (19) allows reciprocal exchange of monomer chains without breaking the tail-to-tail associations, such reciprocal exchanges could result in α and β chains that are linked at their tails but are part of two different tetramers. This situation would not be morphologically detectable (20).

A single 37-nm rod is the most distinctive feature of each junctional complex. The dimensions of the rod and the fact that it appears to nucleate actin polymerization provide evidence that the rod is a short oligomer of F-actin. An actin oligomer of this length would contain 13 actin monomers if the subunits are arranged as in F-actin. The best biochemical estimates for the size of the erythrocyte actin oligomers are based on the total amount of actin per erythrocyte (21) and the number of high-affinity cytochalasin binding sites per cell (22). These estimates indicate a number average of 12–17 actin monomers per oligomer, in close agreement with our morphological observations. The surprisingly regular length of the oligomers (Fig. 3) suggests that there is little variance in the number of monomers per oligomer. The junctional complex may include other proteins that regulate the length of this actin oligomer.

In contrast to Shen *et al.* (11), we have not seen spectrin bound by short globule-like actin oligomers nor have we seen

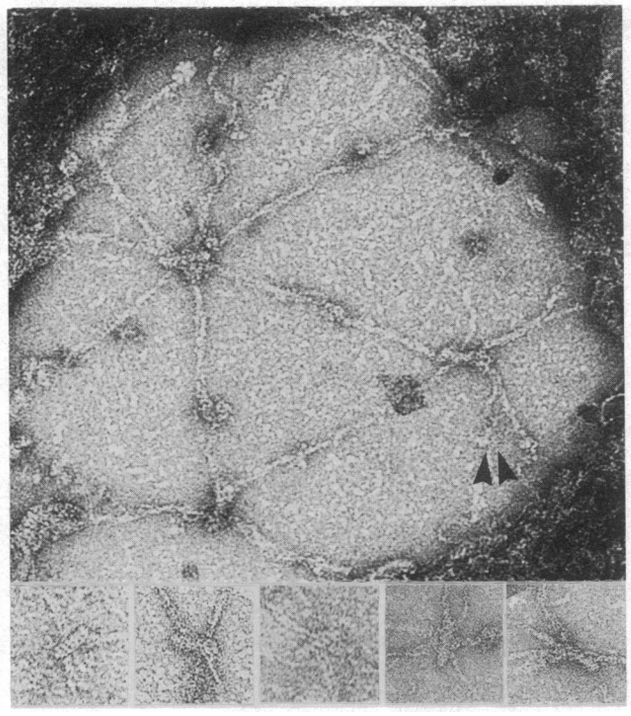

FIG. 3. Junctional complexes. Between four and seven spectrin molecules appear to insert into each junction, but tears (arrowheads) and complete breaks that cannot be detected may exaggerate the number of 4-fold junctions. A repeat pattern is sometimes visible on the junctional rods (*Gallery, Left* and *Middle*). (×200,000.)

oligomers longer than 40 nm binding multiple spectrin clusters of spectrin. Globule-like oligomers as well as longer oligomers with multiple spectrin clusters may arise by breakdown or reannealing of preexisting oligomers during the extensive incubations, density gradient centrifugation, gel filtration, and vacuum dialysis used by Shen *et al.* (11). The actin oligomer is probably not fragmented in the production of our spread preparations because we can identify short rod-like structures with the same dimensions in intact membranes that have not been spread (Fig. 1).

Given 13 monomers per oligomer, the known surface area of an erythrocyte (23), and the measured actin content of an erythrocyte (20), there would be about 250 oligomers/μm^2 in the intact, unspread membrane. In the fully spread preparations, the end-to-end length of the spectrin molecule is about 200 nm, which would give a density of 25–29 oligomers/μm^2 depending on whether one assumes a square or a hexagonal lattice. Thus, the protein density in the spread meshwork must be 9- to 10-fold less than in the intact membrane. The value for the maximum extension ratio of the meshwork would therefore be $(9–10)^{1/2}$, or about 3. Evans and LaCelle (24) determined the relation between erythrocyte membrane stress and strain and found the maximum elastic extension ratio of the erythrocyte membrane to be 3–4.

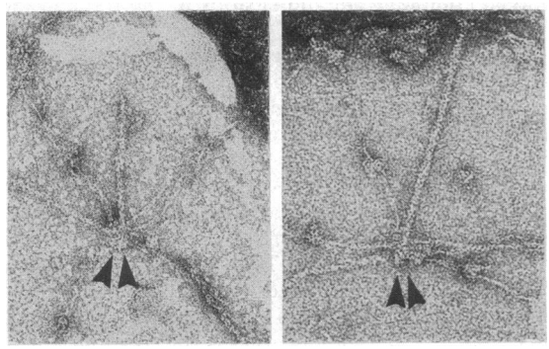

FIG. 4. Actin elongation. When incubated with G-actin, the junctional complexes (arrowheads) served as sites from which actin elongated. (×150,000.)

Only one actin oligomer was seen at each junctional complex in the spread preparations. If band 4.9, the trimeric actin bundling protein of the erythrocyte (25), links several oligomers together such bundled oligomers were either separated as the membrane skeleton was spread or were never included in the spread regions.

We are fairly confident that the unique morphology of spectrin allowed us to correctly identify this molecule in our spread preparations. The identification of the actin oligomers on the basis of the nucleation experiments remains tentative as does the identification of material at the sites we believe represent the occupied ankyrin binding sites on spectrin. Now that we know how to spread the erythrocyte membrane skeleton, direct labeling using a variety of probes is possible and will be required to confirm our tentative assignments, to clarify the relation between the morphology of the spread and the unspread skeleton, and to learn more about the distribution of other known membrane components such as band 4.1, band 4.9 (25), tropomyosin (26), and myosin (27, 28).

We are grateful to Arnljot Elgsaeter and his colleagues for discussions that inspired this work and thank Daniel Kiehart and Carl Cohen for helpful suggestions. Daniel Branton thanks Victor Small, in whose laboratory at the Austrian National Academy of Sciences he completed important preliminary observations. The research was supported by National Institutes of Health Grant HL-17411; T.J.B. was supported by National Institutes of Health NRSA Training Grant 5T32GM07598.

1. Yu, J., Fischman, D. A. & Steck, T. L. (1973) *J. Supramol. Struct.* **1,** 233–248.
2. Sheetz, M. P. & Sawyer, D. (1978) *J. Supramol. Struct.* **8,** 399–412.
3. Tsukita, S., Tsukita, S. & Ishikawa, H. (1980) *J. Cell. Biol.* **85,** 567–576.
4. Tsukita, S., Tsukita, S. & Ishikawa, H. (1984) *J. Cell Biol.* **98,** 1102–1110.
5. Lux, S. E. (1979) *Nature (London)* **281,** 426–429.
6. Branton, D., Cohen, C. M. & Tyler, J. (1981) *Cell* **24,** 24–32.
7. Bennett, V. (1982) *J. Cell Biochem.* **18,** 49–65.
8. Shotton, D. M. (1983) in *Electron Microsopy of Proteins 4*, ed. Harris, J. R. (Academic, London), pp. 205–330.
9. Cohen, C. M. (1983) *Semin. Hematol.* **20,** 141–158.
10. Liu, S.-C., Windisch, P., Kim, S. & Palek, J. (1984) *Cell* **37,** 587–594.
11. Shen, B. W., Josephs, R. & Steck, T. L. (1984) *J. Cell Biol.* **98,** 810–821.
12. Pinder, J. C., Clark, S. E., Baines, A. J., Morris, E. & Gratzer, W. B. (1981) in *The Red Cell: Fifth Ann Arbor Conference*, ed. Brewer, G. J. (Liss, New York), pp. 343–354.
13. Davison, E. & Colquhoun, W. (1985) *J. Electron Microsc. Tech.* **2,** 35–43.
14. Spudich, J. A. & Watt, S. (1971) *J. Biol. Chem.* **246,** 4866–4871.
15. MacLean-Fletcher, S. & Pollard, T. D. (1980) *Biochem. Biophys. Res. Commun.* **96,** 18–27.
16. Shotton, D. M., Burke, B. & Branton, D. (1979) *J. Mol. Biol.* **131,** 303–329.
17. Tyler, J., Hargreaves, W. & Branton, D. (1979) *Proc. Natl. Acad. Sci. USA* **76,** 5192–5196.
18. Morrow, J. S. & Marchesi, V. T. (1981) *J. Cell Biol.* **88,** 463–468.
19. Ungewickell, E. & Gratzer, W. B. (1978) *Eur. J. Biochem.* **88,** 379–385.
20. Stokke, B. T. (1984) Dissertation (The University of Trondheim, Trondheim, Norway).

21. Pinder, J. C. & Gratzer, W. B. (1983) *J. Cell Biol.* **96,** 768–775.
22. Lin, D. C. & Lin, S. (1978) *J. Biol. Chem.* **253,** 1415–1419.
23. Ponder, E. (1948) *Hemolysis and Related Phenomena* (Grune & Stratton, New York).
24. Evans, E. A. & LaCelle, P. L. (1975) *Blood* **45,** 29–43.
25. Siegel, D. L. & Branton, D. (1985) *J. Cell Biol.* **100,** 775–785.
26. Fowler, V. M. & Bennett, V. (1984) *J. Biol. Chem.* **259,** 5978–5989.
27. Fowler, V. M., Davis, J. Q. & Bennett, V. (1985) *J. Cell Biol.* **100,** 47–55.
28. Wong, A. J., Kiehart, D. P. & Pollard, T. P. (1985) *J. Biol. Chem.* **260,** 46–49.